

Single-Event Effects Test Report of the LMH5401-SP 8-GHz, Low Noise, Low Power, Fully-Differential Amplifier

ABSTRACT

The effect of heavy-ion irradiation on the single-event effects performance of the LMH5401-SP high-performance, differential amplifier is summarized in this report. Heavy-ions with an LET_{EFF} up to 83.21 MeV-cm²/mg were used to irradiate two production devices in 45 runs. Flux up to 10⁵ ions/cm²-s and fluences up to 10⁷ ions/cm² at temperatures of 25°C (SET) and 125°C (SEL), were used for the characterization. Results demonstrate that the LMH5401-SP is SEL-free up to $LET_{EFF} = 83.21$ MeV-cm²/mg and 125°C, and the cross section for the SET is discussed.

Contents

1	Overview	3
2	Single-Event Effects	3
3	Test Device and Evaluation Board Information	4
4	Irradiation Facility and Setup	6
5	Depth, Range, and LET_{EFF} Calculation	7
6	Test Set-Up and Procedures	7
7	Single-Event Latch-up (SEL) Results	10
8	Single-Event Transients (SET) Results	11
9	Event Rate Calculations	18
10	Summary	19
Appendix A	Total Ionizing Dose from SEE Experiments	20
Appendix B	Confidence Interval Calculations	21
Appendix C	Orbital Environment Estimations	23
Appendix D	References	25

List of Figures

1	Decapped LMH5401-SP (Left) and Device Block Diagram (Right)	4
2	LMH5401EVM-CVAL Board Top View (Left) and Bottom View (Right)	4
3	LMH5401EVM-CVAL, Evaluation Module Board Schematic for SEE Testing	5
4	LMH5401-SP Evaluation Board Mounted in Front of the Heavy-Ion Beam Exit Port	6
5	GUI of RADsim Application Used to Determine Key Ion Parameters	7
6	Block Diagram of the Test Setup Used for the LMH5401-SP Mounted on a LMH5401EVM-CVAL SEE Characterization	9
7	Current and Temperature vs Time Data for V_{S+} and V_{S-} During SEL Run #1 on the LMH5401-SP	11
8	Worst Case Positive Voltage Excursion Upset on Run # 13 at $LET_{EFF} = 83.21$ MeV-cm ² /mg	14
9	Worst Case Negative Voltage Excursion Upset on Run # 23 at $LET_{EFF} = 83.21$ MeV-cm ² /mg	14
10	Histogram of the Maximum Voltage for Each Upset Recorded	15
11	Histogram of the Minimum Voltage for Each Upset Recorded	15
12	Histogram of the Transient Recovery Time for Each Upset Recorded	16
13	Cross Section and Weibull-Fit for the DC Test at Supply Voltages of ± 1.65 V	16
14	Cross Section and Weibull-Fit for the DC Test at Supply Voltages of ± 2.5 V	17
15	All V_{OUT} -Differential AC Upsets	18

16	Worst Case Upset on AC Mode When Monitoring Each Output Leg of the LMH5401-SP Separately	18
17	Integral Particle Flux vs LET _{EFF}	23
18	Device Cross-Section vs LET _{EFF}	24

List of Tables

1	Overview Information.....	3
2	LET _{EFF} , Depth and Range for the Ions Used for SEE Characterization of the LMH5401-SP	7
3	Equipment Set Up and Parameters Used for the SEL Testing the LMH5401-SP	8
4	Summary of LMH5401-SP SEL Results	10
5	Summary of the LMH5401-SP DC Tests at ± 1.65 V	12
6	Summary of the LMH5401-SP DC Tests at ± 2.5 V.....	12
7	Summary of the LMH5401-SP AC Tests at ± 1.65 V	13
8	Summary of the LMH5401-SP AC Tests at ± 2.5 V.....	13
9	Weibull-FIT Parameters for DC Test at Supply Voltages of ± 1.65 and ± 2.5 V	17
10	SEL Event Rate Calculations for Worst-Week LEO and GEO Orbits	19
11	SET Event Rate Calculations DC ± 1.65 Supply Voltage for Worst-Week LEO and GEO Orbits.....	19
12	SET Event Rate Calculations DC ± 2.5 Supply Voltage for Worst-Week LEO and GEO Orbits	19
13	Experimental Example Calculation of Mean-Fluence-to-Failure (MFTF) and σ Using a 95% Confidence Interval	22

Trademarks

DuPont, Kevlar are registered trademarks of E.I. du Pont de Nemours and Company.
 LabView is a trademark of National Instruments Corporation.
 All other trademarks are the property of their respective owners.

1 Overview

The LMH5401-SP is a very high-performance, differential amplifier optimized for radio frequency (RF), intermediate frequency (IF), or high-speed, DC-coupled, time-domain applications. The device is ideal for DC- or AC-coupled applications that may require a single-ended-to-differential (SE-DE) conversion when driving an analog-to-digital converter (ADC). The LMH5401-SP generates very low 2nd and 3rd order distortion when converting from SE to DE or DE-DE (differential-to-differential), making it an ideal replacement for high performance balun. The device incorporates a common-mode reference input that aligns the amplifier output common-mode with the analog to digital converter (ADC) inputs requirements. The LMH5401-SP offers a 8-GHz gain bandwidth product (GBP). [Table 1](#) lists the general device information and test conditions.

For more detailed technical specifications, user-guides, and application notes visit:
<http://www.ti.com/product/LMH5401-SP>.

Table 1. Overview Information

Description	Device Information
TI Part Number	LMH5401-SP
SMD Number	5962-1721401VXC
Device Function	Fully Differential Amplifier
Technology	CBiCMOS
Exposure Facility	Radiation Effects Facility, Cyclotron Institute, Texas A&M University
Heavy-Ion Fluence per Run	10 ⁶ (SET)– 10 ⁷ (for SEL and SET) ions/cm ²
Irradiation Temperature	25°C and 125°C (for SEL testing)

2 Single-Event Effects

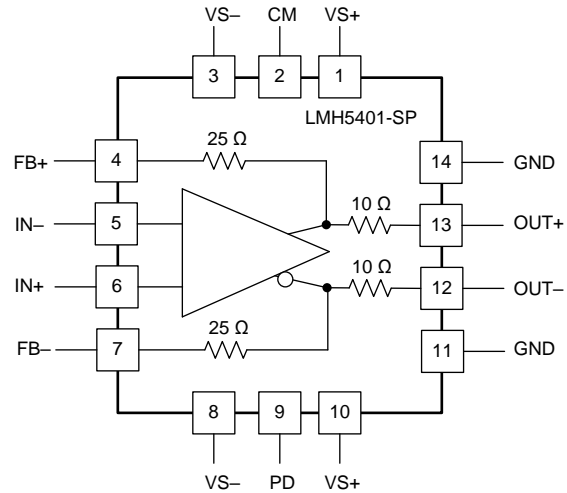
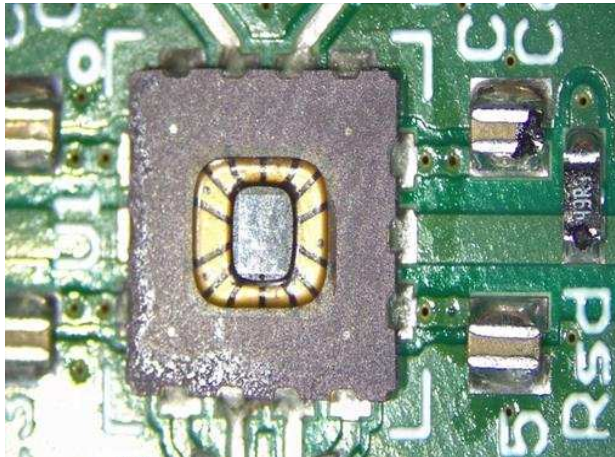
The primary concern for the LMH5401-SP are its resilience against the destructive single-event effects (DSEE), such as single-event latch-up (SEL) and single-event-burnout (SEB). Since the operating voltage of LMH5401-SP is low, SEB is not a concern.

The LMH5401-SP was characterized for SEL events. In mixed technologies, such as the CBi-CMOS process used for the LMH5401-SP, the presence of the CMOS circuitry introduces a potential SEL susceptibility. SEL can occur if excess current injection caused by the passage of an energetic ion is high enough to trigger the formation of a parasitic cross-coupled PNP and NPN bipolar structure (formed between the p-substrate and n-well and n+ and p+ contacts) [1][2]. If formed, the parasitic bipolar structure creates a high-conductance path (creating a steady-state current that is orders-of-magnitude higher than the normal operating current) between power and ground that persists (is "latched") until power is removed or until the device is destroyed by the high-current state. The LMH5401-SP exhibited absolutely no SEL with heavy-ions of up to LET_{EFF} = 83.21 MeV-cm²/mg at fluences in excess of 10⁷ ions/cm² and a die temperature of 125°C.

Another concern on high reliability and performance applications is the single-events-transient (SET) characteristic of the device. The LMH5401-SP SET performance was characterized up to LET_{EFF} = 83.21 MeV-cm²/mg. The device was characterized for SET at supply voltages of ±1.65 and ±2.5 V under AC and DC input conditions. Test conditions and results are discussed in [Section 8](#).

3 Test Device and Evaluation Board Information

The LMH5401-SP is packaged in a 14-pin, thermally-enhanced, leadless ceramic chip carrier package (LCCC) as shown in Figure 1. The LMH5401EVM-CVAL evaluation board was used to evaluate the single-events-effects (SEE) of the LMH5401-SP. Top and bottom views of the evaluation board used for the radiation testing are shown in Figure 2. Schematic of the evaluation board used for radiation testing is shown in Figure 3. For more technical information about the LMH5401-SP, see <https://www.ti.com/product/LMH5401-SP/technicaldocuments>.



Copyright © 2018, Texas Instruments Incorporated

Figure 1. Decapped LMH5401-SP (Left) and Device Block Diagram (Right)

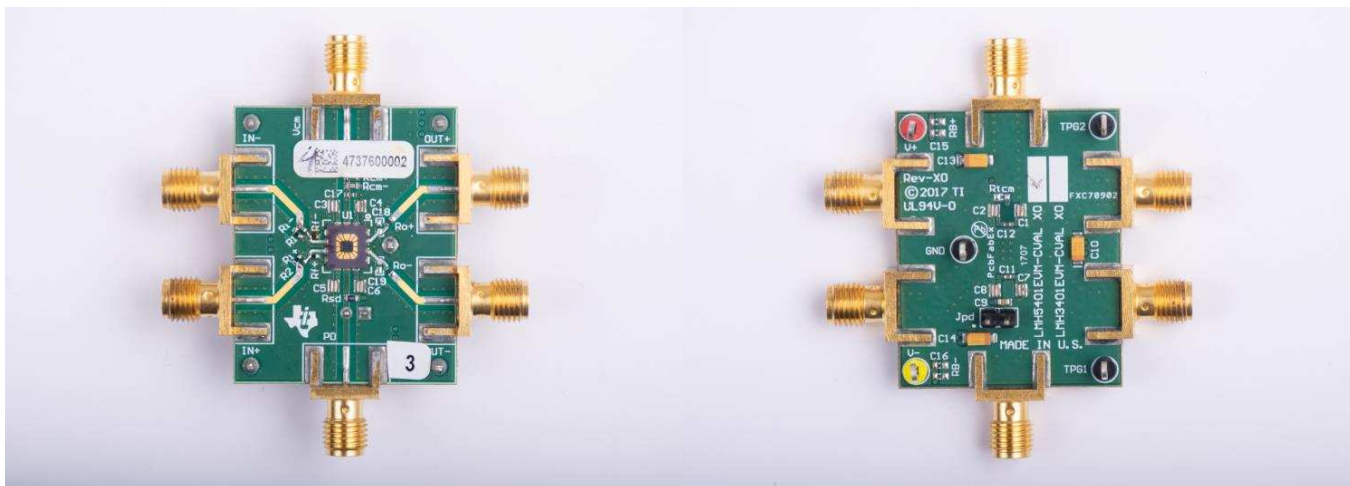


Figure 2. LMH5401EVM-CVAL Board Top View (Left) and Bottom View (Right)

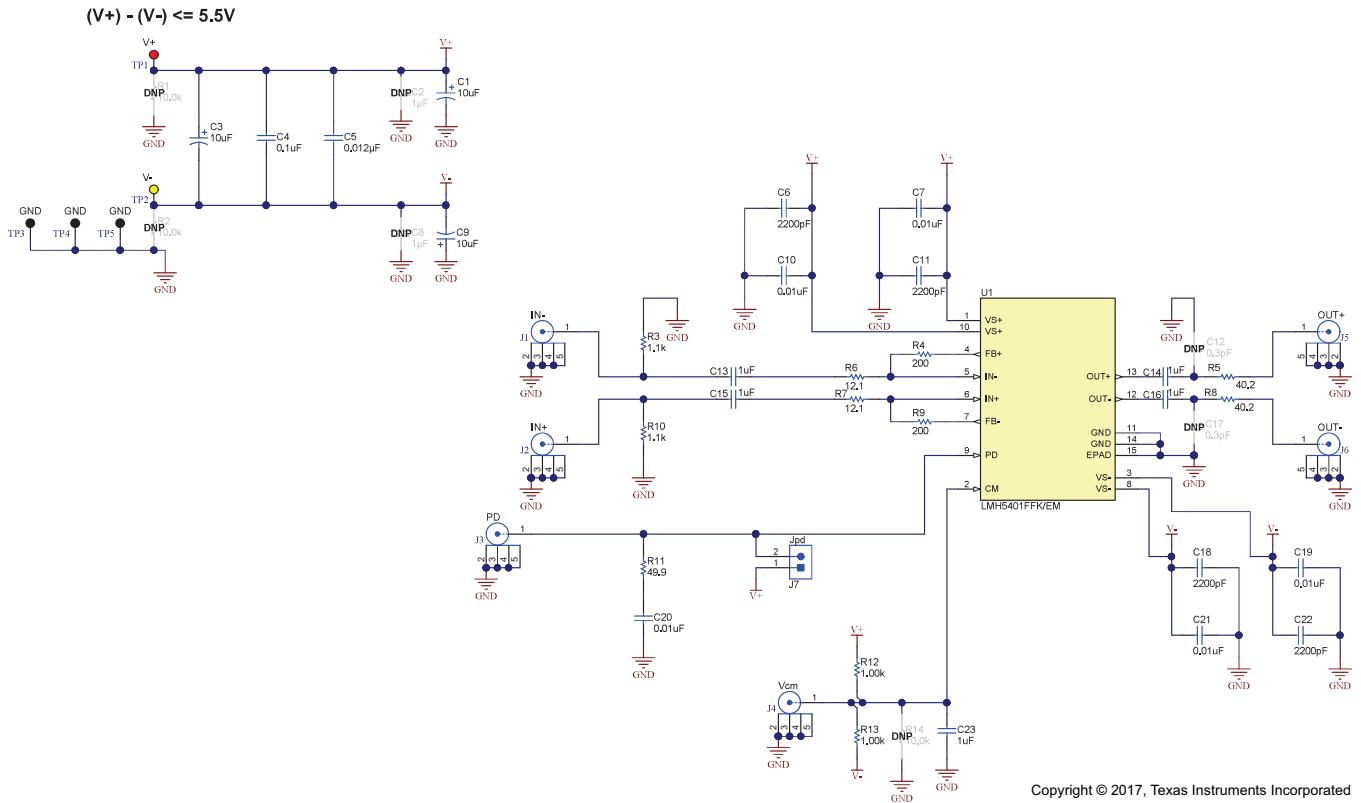


Figure 3. LMH5401EVM-CVAL, Evaluation Module Board Schematic for SEE Testing

4 Irradiation Facility and Setup

The heavy-ion species used for the SEE studies on this product were provided and delivered by the TAMU Cyclotron Radiation Effects Facility [3], using a superconducting cyclotron and advanced electron cyclotron resonance (ECR) ion source. At the fluxes used, ion beams had good flux stability and high-irradiation uniformity over a 1-in diameter circular cross-sectional area for the in-air station. Uniformity is achieved by means of magnetic defocusing. The flux of the beam is regulated over a broad range spanning several orders of magnitude. For the bulk of these studies ion fluxes between 10^4 and 10^5 ions/s- cm^2 were used to provide a heavy-ion fluences between 10^6 and 10^7 ions/ cm^2 .

For these experiments Praseodymium (^{141}Pr), Krypton (^{84}Kr), and Copper (^{63}Cu) were used. Angles were used to increment the LET_{EFF} , details are provided in Section 5. The ^{141}Pr , ^{84}Kr , and ^{63}Cu ions used had a total kinetic energy of 2114, 1259, and 944 MeV in the vacuum, (15-MeV/amu line) respectively. Ion beam uniformity for all tests was in the range of 88 to 97%.

Figure 4 shows the LMH5401-SP mounted on the LMH5401EVM-CVAL board in front of the beam exit port, as in the heavy-ion characterization. The beam port has a 1-mil Aramite (Kevlar®), 1-in diameter to allow in-air testing while maintaining the vacuum in the accelerator with only minor ion energy losses. The air space between the DUT and beam exit port the was set to 40 mm (most used) and 60 mm.

The data recorded in this report was based on finalized EVM boards with optimized component values that follow data sheet recommendations.

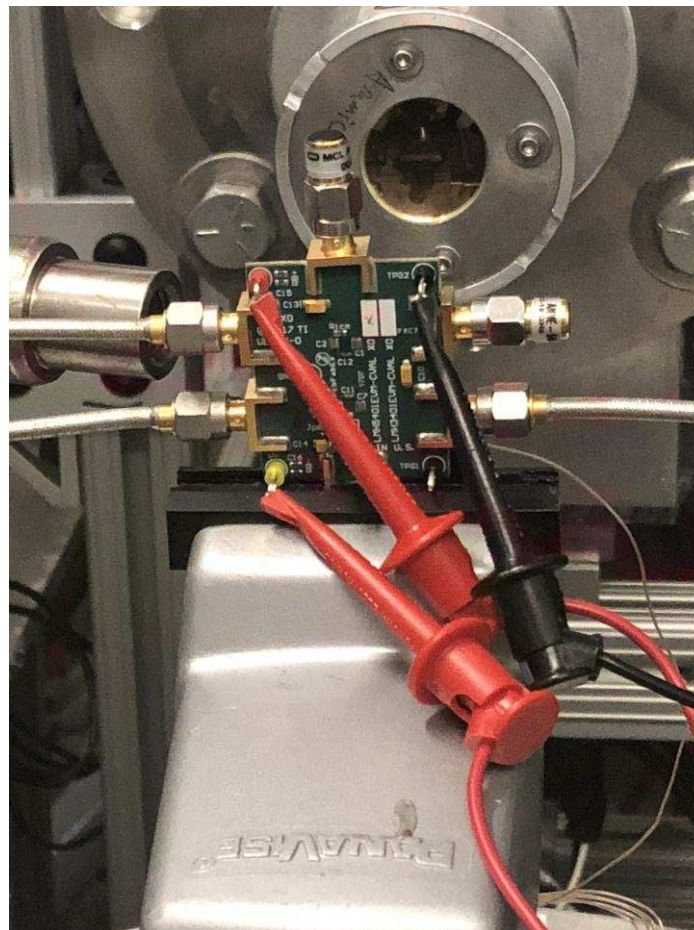


Figure 4. LMH5401-SP Evaluation Board Mounted in Front of the Heavy-Ion Beam Exit Port

5 Depth, Range, and LET_{EFF} Calculation

The LMH5401-SP is fabricated in the TI CBiCMOS process and the die is packaged as a flip chip. The decapped unit exposes the silicon substrate directly when packaged in the flip-chip configuration. The units used were backgrounded to 52.6 microns, for proper ion penetration. The effective LET (LET_{EFF}), depth and range was determined with the custom RADsim-IONS application (developed at Texas Instruments and based on the latest SRIM2013 [4] models). The applications accounts for energy loss through the 1-mil thick Aramica (DuPont® Kevlar®) beam port window and the air gap between the DUT and the heavy-ion exit port (40 mm and 60 mm). An image of the RADsim - IONS is shown in Figure 5 and the ions details are presented in Table 2.

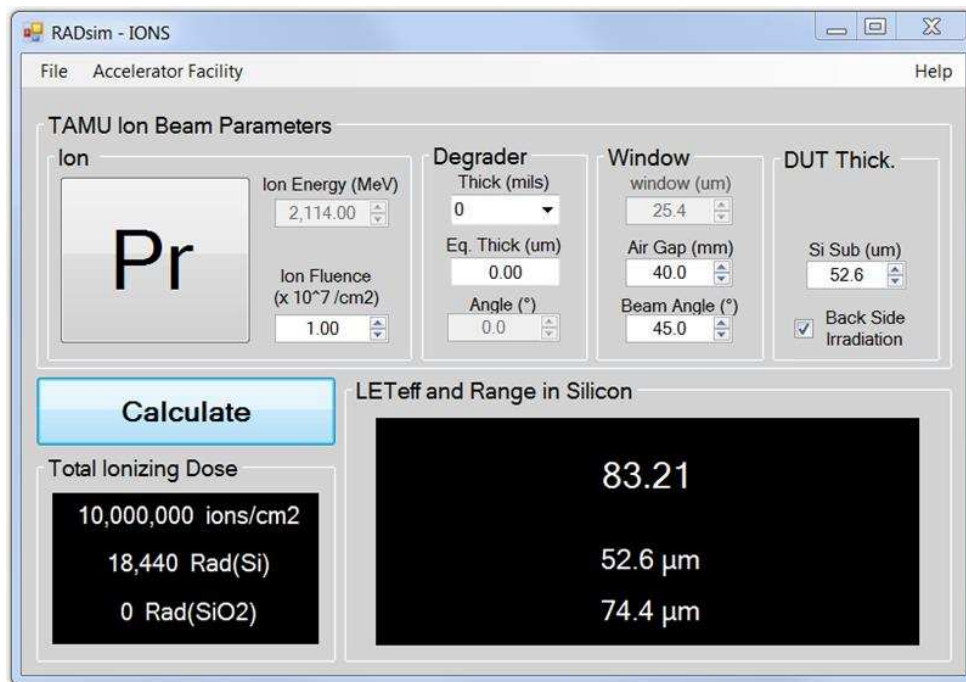


Figure 5. GUI of RADsim Application Used to Determine Key Ion Parameters

Table 2. LET_{EFF}, Depth and Range for the Ions Used for SEE Characterization of the LMH5401-SP

Ion Type	Angle of Incidence (°)	Depth in Silicon (μm)	Range in Silicon (μm)	LET _{EFF} (MeV-cm ² /mg)	Distance (mm)
Cu	10	52.6	53.4	25.40	40
Cu	20	52.6	56	27.02	40
Cu	30	52.6	60.7	30.17	40
Kr	0	52.6	52.6	36.49	40
Kr	30	52.6	60.7	43.60	40
Pr	45	52.6	74.4	48.93	60
Pr	0	52.6	52.6	64.59	60
Pr	0	52.6	52.6	70.49	40
Pr	45	52.6	74.4	83.21	40

6 Test Set-Up and Procedures

SEE testing was performed on a LMH5401-SP device mounted on a LMH5401EVM-CVAL. The device was provided power through the V_S+/V_S- (±2.5 and ±1.65 V) and GND inputs (TP1, TP2 and TP3) using the N6702 precision power supply in a 4-wire configuration. The LMH5401-SP was evaluated with a DC and AC input signal provided on the IN+ input. For the AC test, the input was driven onto the IN+ pin (J2) with an Agilent/HP 8665B signal generator (capable of providing a 6-GHz signal) using a high speed

coaxial cable model: S141MMHF-36-2. Input frequency was set to 1 (most used) and 2 GHz, the input amplitude was set in such way that the output was set to 500 mV_{P-P} (most used) and 1 V_{P-P}. For the DC test, the IN+ was connected to GND with a 50-Ω high speed termination SMA (on the J2 connector). For both DC and AC test, the IN- (J3 connector) was connected to GND using a high speed SMA 50-Ω termination. Also during all time the PD pin (J3 connector) was connected to GND using a 50-Ω high speed termination.

The devices was evaluated on differential mode. SETs where monitored using a DPO7254C Digital Phosphor Oscilloscope (4 ch, 2.5-GHz BW and 40-GS/s Sample Rate). The output of the LMH5401-SP was monitored in two different ways, named here as:

- Single-Ended (SE)
- Differential-Ended (DE)

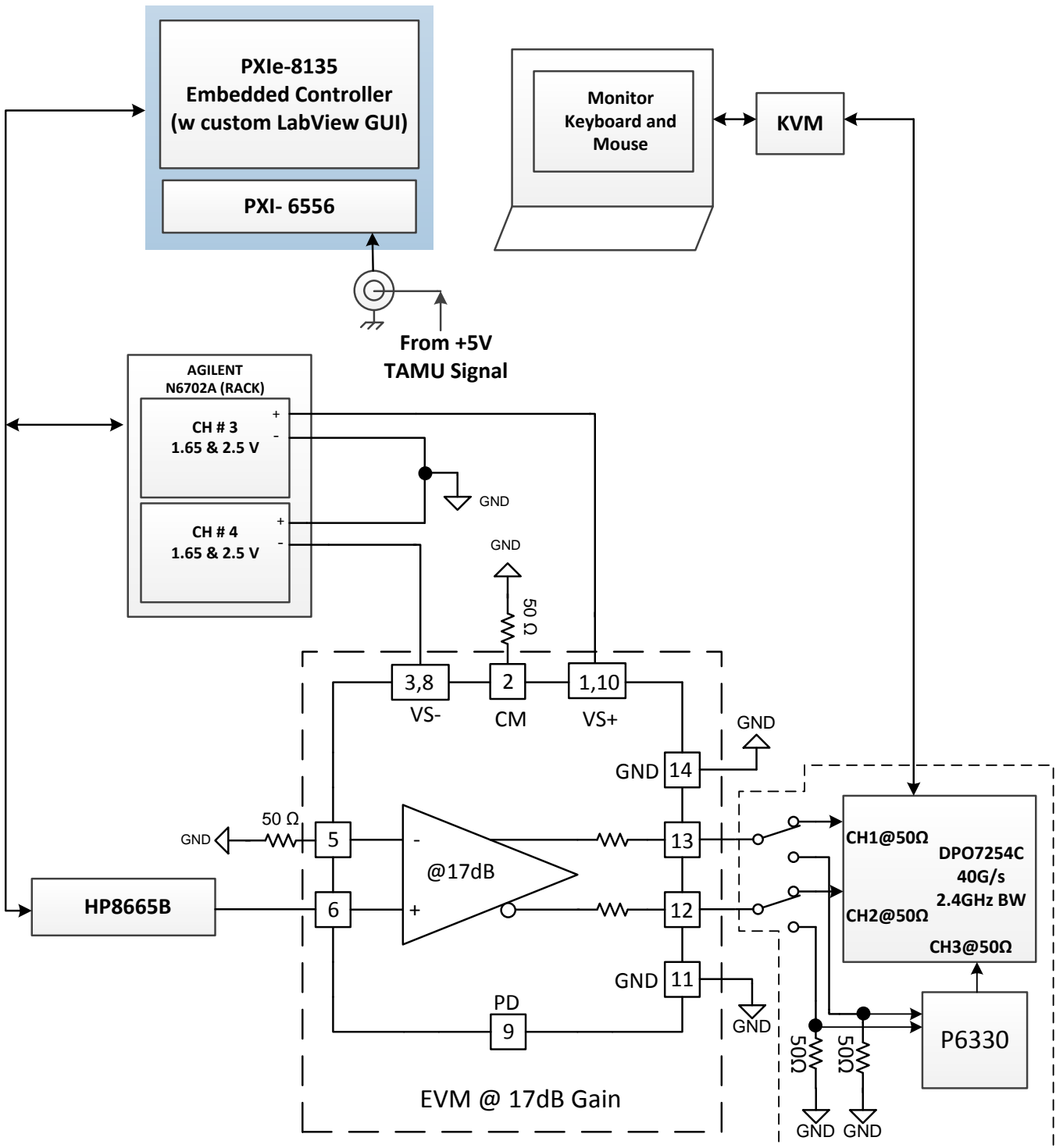
For the SE case, the outputs were monitored and terminated individually to 50 Ω on the scope. On the DE mode, the outputs were terminated to 50 Ω and the differential signal was monitored using a P6330 High Speed probe (BW > 3 GHz). When the P6330 differential probe is connected to the scope, the input impedance of the scope is set to 50-Ω automatically, for impedance matching between the probe output and the scope. However the probe input is high impedance (HZ). The DPO was used to monitor the output voltage and capture any SET that exceed the limits set for the window trigger. The scope has a 3.2-μs update rate under the conditions used when collecting data (Fast-Frame mode). The update rate represents the amount of time to re-arm the scope trigger after an upset.

The power supply (PS) was controlled and monitored using a custom-develop LabView™ program (PXI-RadTest) running on a NI-PXIe-8135 controller. The Agilent/HP 8665B was controlled via the GPIB bus, using the stand alone LabView™ drivers were used to control it. The DPO7254C was controlled using it front-panel interface. The DPO was left in the cave at all times, to minimize the probe cable length. A KVM extender was used to control and view the DPO from the control room at TAMU. A block diagram of the setup used for SEE testing the LMH5401-SP is illustrated in Figure 6. Equipment settings and compliances used during the characterization are shown in Table 3. For the SEL testing the device was heated using a convection heat gun aimed at the die. The junction temperature was monitored by using a K-type thermocouple attached as close as possible to the die.

Table 3. Equipment Set Up and Parameters Used for the SEL Testing the LMH5401-SP

Pin Name	Equipment Used	Capability	Compliance	Range of Values Used
V _{s+} /V _{s-}	Agilent N6702A	5 A	5 A	±1.65 ,±2.5 and ±2.75V
IN+	Agilent/HP 8665B	6 GS/s	—	0.30, 1 and 2 GS/s
OUT+ and OUT-	Tektronix DPO7104C	40 GS/s	—	20 GS/s
OUT+ and OUT-	P6330	BW > 3 GHz	—	2.4 GHz (DPO BW)

All boards used for SEL testing were fully checked for functionality and dry runs performed to ensure that the test system was stable under all bias and load conditions prior to being taken to the TAMU facility. During the heavy-ion testing, the LabView™ control program powered up the LMH5401-SP device and set the external sourcing and monitoring functions of the external equipment. After functionality and stability had been confirmed, the beam shutter was opened to expose the device to the heavy-ion beam. The shutter remained open until the target fluence was achieved (determined by external detectors and counters).



The SPDT connections shown in the block diagram was not physically present at any time, rather is used to represent the SE and DE connections using one block diagram.

Figure 6. Block Diagram of the Test Setup Used for the LMH5401-SP Mounted on a LMH5401EVM-CVAL SEE Characterization

7 Single-Event Latch-up (SEL) Results

All SEL characterizations were performed with forced hot air to maintain the die temperature at 125°C during the tests. The device was exposed to a Praseodymium (Pr) heavy-ion beam incident on the die surface at 45° for an effective LET of 83.21 MeV-cm²/mg. A flux of 10⁵ ions/cm²-s and fluence of 10⁷ ions/cm² per run was used in all three runs. The device was power up with the recommended voltage of ±2.5 V and recommended maximum voltage of ±2.75 V. During the first three runs the device was actively amplifying a single ended input signal of -6 dBm at 1 GHz. Both differential outputs were independently terminated (SE) at 50 Ω on the scope. Under this conditions the output was set to 250-mV_{P.P} SE (500 mV_{P.P} on DE), and the V_{IN} = ±2.5 V. Run number four was run at input frequency of 30 MHz, with V_{IN} set to ±2.75-V. The input signal voltage to the IN+ was set to 286 mV, given an output of 1 V_{P.P} (recommended max output voltage). The device was set on a SE-DE mode, with each output leg terminated to 50 Ω on the scope.

Time duration to achieve this fluence was approximately 2 minutes. The SEL results and conditions are summarized in [Table 4](#). No SEL events were observed under any of the three test runs, indicating that the LMH5401-SP is SEL-immune at T = 125°C and LET = 83.21 MeV-cm²/mg. A typical temperature and current vs time plot is shown on [Figure 7](#).

Table 4. Summary of LMH5401-SP SEL Results⁽¹⁾

Run #	Unit #	Temp (°C)	Ion Type	Incident Angle (°)	Fluence (ions/cm ²)	VS (±V)	Input Frequency (GHz)	Load _{PEROUTPUT} (Ω)	Output Differential (mV _{PP})	SEL Events
1	2	125	Pr	45	1.0 × 10 ⁷	2.5	1	50	500	0
2	2	125	Pr	45	1.0 × 10 ⁷	2.5	1	50	500	0
3	2	125	Pr	45	1.0 × 10 ⁷	2.5	1	50	500	0
4	3	125	Pr	45	3.0 × 10 ⁷	2.75	0.03	50	1	0

⁽¹⁾ SEL results with T = 125°C and LET_{EFF} = 83.21 MeV-cm²/mg.

The upper-bound SEL cross-sections was calculated based on 0 events observed. Only run # 4 was used for the cross section calculation since this was the run with the device power up to the maximum recommended voltage. Using the MTBF method at 95% confidence interval (see [Appendix B](#) for a discussion of the MTBF cross section calculation method), the combined upper bound cross section is:

$$\sigma_{\text{SEL}} \leq 1.23 \times 10^{-7} \text{ cm}^2/\text{device at LET}_{\text{EFF}} = 83.2 \text{ MeV-cm}^2/\text{mg, } V_{\text{IN}}=\pm 2.75\text{-V, } T = 125^\circ\text{C and 95\% conf.} \quad (1)$$

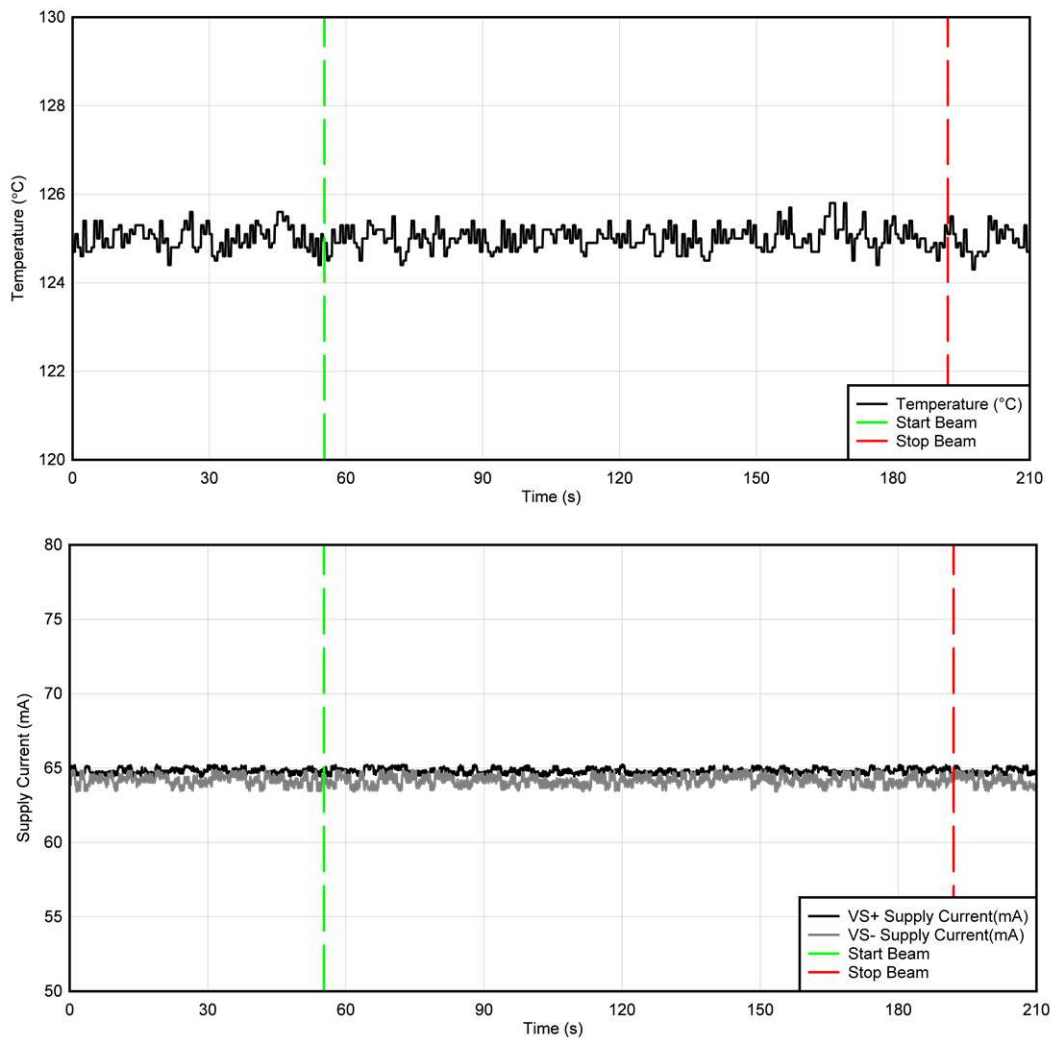


Figure 7. Current and Temperature vs Time Data for V_{S+} and V_{S-} During SEL Run #1 on the LMH5401-SP

8 Single-Event Transients (SET) Results

The LMH5401-SP was characterized for SETs from 25.4 to 83.21 MeV-cm²/mg (refer to Table 2) at ±1.65- and ±2.5-V supply voltages. The device was tested at room temperature for all SETs runs. Since the LMH5401-SP is a flip chip the devices were thinned to 52.6 μm for proper heavy-ion penetration into the active circuits. Flux of 10⁴ and 10⁵ (most used) ions/cm²-s and fluences of 10⁶ and 10⁷ (most used) ions/cm² per run were used during the heavy ion characterization. The devices were tested under static (DC) and dynamic (AC) inputs (as described in Section 6), on a voltage gain of 17 dB (under these conditions the device has the flattest frequency response). The SETs discussed on this report were defined as output voltage excursions that exceed a window trigger set on the DPO7104C. Outputs of the LMH5401-SP were monitored individually (SE) or differentially (DE), under both conditions each leg of the differential outputs was terminated at 50 Ω. Test conditions used during the testing are presented in Table 5 to Table 8. Positive and negative upsets excursions were observed under DC test. Figure 8 shows the worst case positive voltage excursion upset and Figure 9 shows the worst case negative voltage excursion. These plots represent the worst case voltage excursions for all data collected. As expected the longer voltage excursions will result in the longer transient recovery time (~3 ns), as observed on Figure 9. For each upset the maximum, minimum and transient recovery time was recorded and shown as a histogram in Figure 10 to Figure 12. Weibull-Fit and cross section for the DC test at ±1.65- and ±2.5-V supply voltages are presented on Figure 13 and Figure 14 respectively. The Weibull equation used for the fit is presented in Equation 2, and parameters are shown in Table 9. To calculate the cross section values

at the different supply voltages the total number of upsets (or transients) and the fluences were combined (add together) by LET_{EFF} to calculate the upper bound cross section (as discussed in [Appendix B](#)) at 95% confidence interval. The $\sigma_{PERCASE}$ cross section presented on the summary tables, was calculated using the MTBF method at 95% confidence. For the AC test, not a single upset exceeded the ± 536 -mV window trigger when monitoring the outputs on differential mode. However some upsets were observed when setting the trigger to ± 268 mV and monitoring each output individually. When observing the upsets, both outputs legs (inverting and non-inverting) track each other for most of the time. Since both legs track each other differentially the upset is cancelled. All detected AC upsets when monitoring the outputs individually were converted to differential and are shown in [Figure 15](#). Worst case AC upset for each leg is shown in [Figure 16](#). It is important to notice that **any SET** with rail saturation was observed under the DC or AC testing.

The upper-bound SET cross-sections (σ_{ALL}) was calculated based using the combined (add together) events and fluences. Using the MTBF method at 95% confidence interval (see [Appendix B](#) for a discussion of the MTBF cross section calculation method), the combined upper bound cross section is:

$$\sigma_{SET-ALL-DC} \leq 3.91 \times 10^{-6} \text{ cm}^2/\text{device at LET} = 83.2 \text{ MeV}\cdot\text{cm}^2/\text{mg, T} = 25^\circ\text{C, 95\% conf. and } V_s = \pm 1.65 \text{ V.}$$

$$\sigma_{SET-ALL-DC} \leq 3.08 \times 10^{-6} \text{ cm}^2/\text{device at LET} = 83.2 \text{ MeV}\cdot\text{cm}^2/\text{mg, T} = 25^\circ\text{C, 95\% conf. and } V_s = \pm 2.5 \text{ V.}$$

$$\sigma_{SET-ALL-AC-DIFF} \leq 4.94 \times 10^{-8} \text{ cm}^2/\text{device at LET} = 83.2 \text{ MeV}\cdot\text{cm}^2/\text{mg, T} = 25^\circ\text{C, 95\% conf. and } V_s = \pm 1.65 \text{ V.}$$

Table 5. Summary of the LMH5401-SP DC Tests at ± 1.65 V

Run #	Unit #	Distance (mm)	LETEFF (MeV·cm ² /mg)	Flux (ions/cm ² ·s)	Fluence (ions/cm ²)	Trigger Value	SET _{DIFF} Events	$\sigma_{PERCASE}$ @ 95% (cm ² /device)
5	2	40	27	9.64E+04	1.00E+07	LL = -80 mV; UL = 120 mV	0	4.92312E-08
6	2	40	27	8.87E+04	9.96E+06	LL = -80 mV; UL = 120 mV	0	4.95772E-08
7	2	40	30.17	1.03E+05	9.97E+06	LL = -80 mV; UL = 120 mV	0	4.95076E-08
8	2	40	30.17	1.04E+05	1.00E+07	LL = -80 mV; UL = 120 mV	1	4.98466E-08
9	2	40	36.49	1.03E+05	1.00E+07	LL = -80 mV; UL = 120 mV	0	4.92803E-08
10	2	40	36.49	9.69E+04	9.98E+06	LL = -80 mV; UL = 120 mV	1	5.01064E-08
11	2	40	43.6	8.63E+04	9.98E+06	LL = -80 mV; UL = 120 mV	1	5.00813E-08
12	2	60	48.93	1.13E+05	9.98E+06	LL = -80 mV; UL = 120 mV	3	5.00952E-08
13	2	60	64.59	1.14E+05	1.01E+07	LL = -80 mV; UL = 120 mV	5	4.97512E-08
14	3	40	83.21	1.04E+05	1.00E+07	LL = -80 mV; UL = 120 mV	27	4.98504E-0

Table 6. Summary of the LMH5401-SP DC Tests at ± 2.5 V

Run #	Unit #	Distance (mm)	LETEFF (MeV·cm ² /mg)	Flux (ions/cm ² ·s)	Fluence (ions/cm ²)	Trigger Value	SET _{DIFF} Events	$\sigma_{PERCASE}$ @ 95% (cm ² /device)
15	2	40	30.17	1.02E+05	1.00E+07	LL = -80 mV; UL = 120 mV	0	4.91822E-08
16	2	40	30.17	9.95E+04	1.00E+07	LL = -80 mV; UL = 120 mV	0	4.91822E-08
17	2	40	36.49	9.87E+04	1.00E+07	LL = -80 mV; UL = 120 mV	0	4.93789E-08
18	2	40	36.49	9.52E+04	1.00E+07	LL = -80 mV; UL = 120 mV	0	4.92803E-08
19	2	40	43.6	8.06E+04	1.00E+07	LL = -80 mV; UL = 120 mV	3	4.98504E-08

Table 6. Summary of the LMH5401-SP DC Tests at ±2.5 V (continued)

Run #	Unit #	Distance (mm)	LETEFF (MeV·cm ² /mg)	Flux (ions/cm ² ·s)	Fluence (ions/cm ²)	Trigger Value	SET _{DIFF} Events	σ _{PERCASE} @ 95% (cm ² /device)
20	2	60	48.93	1.13E+05	9.97E+06	LL = -80 mV; UL = 120 mV	9	5.01605E-08
21	3	60	64.59	1.01E+05	1.00E+07	LL = -80 mV; UL = 120 mV	16	4.98504E-08
22	2	60	64.59	1.15E+05	1.00E+07	LL = -80 mV; UL = 120 mV	14	4.98504E-08
23	3	40	70.49	9.51E+04	1.01E+07	LL = -80 mV; UL = 120 mV	7	4.97512E-08
24	3	40	83.21	1.01E+05	1.00E+07	LL = -80 mV; UL = 120 mV	20	4.995E-08
25	3	60	64.59	1.01E+05	9.99E+06	LL = -80 mV; UL = 120 mV	13	5.0035E-08
26	3	40	70.49	1.02E+05	9.96E+06	LL = -80 mV; UL = 120 mV	11	5.01857E-08

Table 7. Summary of the LMH5401-SP AC Tests at ±1.65 V

Run #	Unit #	Distance (mm)	LETEFF (MeV·cm ² /mg)	Flux (ions/cm ² ·s)	Fluence (ions/cm ²)	Vout (VP-P)	Input Frequency (GHz)	Trigger Value (V)	SET _{DIFF} Events	σ _{PERCASE} @ 95% (cm ² /device)
27	2	40	27	9.21E+04	9.98E+06	0.5	1	±0.536	0	4.94878E-08
28	2	40	27	9.61E+04	9.98E+06	0.5	1	±0.536	0	4.94878E-08
29	2	40	30.17	9.72E+04	9.98E+06	0.5	1	±0.536	0	4.94927E-08
30	2	40	30.17	9.41E+04	9.96E+06	0.5	2	±0.536	0	4.95573E-08
31	2	40	36.49	9.43E+04	1.01E+07	0.5	1	±0.536	0	4.91332E-08
32	3	60	64.59	9.17E+03	1.00E+06	1	1	±0.536	0	4.92803E-07
33	3	60	64.59	9.07E+03	1.00E+06	1	1	±0.536	0	4.91822E-07
34	3	60	64.59	1.05E+05	9.96E+06	1	1	±0.268	0	4.95672E-08
35	3	60	64.59	1.02E+05	1.00E+07	1	2	±0.536	0	4.94036E-08
36	3	40	70.49	9.93E+04	9.96E+06	1	2	±0.536	0	4.95921E-08
37	3	40	83.21	1.00E+05	9.99E+06	1	2	±0.536	0	4.94283E-08

Table 8. Summary of the LMH5401-SP AC Tests at ±2.5 V

Run #	Unit #	Distance (mm)	LETEFF (MeV·cm ² /mg)	Flux (ions/cm ² ·s)	Fluence (ions/cm ²)	Vout (VP-P)	Input Frequency (GHz)	Trigger Value	SET _{DIFF} Events	σ _{PERCASE} @ 95% (cm ² /device)
38	2	40	25.4	9.84E+04	1.00E+07	0.5	1	±0.536	0	4.93789E-08
39	2	40	25.4	9.69E+04	1.00E+07	0.5	1	±0.536	0	4.92312E-08
40	2	40	27	8.84E+04	1.00E+07	0.5	1	±0.536	0	4.93789E-08
41	2	40	30.17	9.72E+04	9.97E+06	0.5	1	±0.536	0	4.95324E-08
42	2	40	30.17	9.77E+04	1.00E+07	0.5	2	±0.536	0	4.91822E-08
43	2	40	36.49	9.75E+04	9.96E+06	0.5	1	±0.536	4	5.02109E-08
44	3	60	64.59	1.05E+05	9.96E+06	1	1	±0.536	0	4.95722E-08
45	3	60	64.59	1.04E+05	9.98E+06	1	2	±0.536	0	4.94927E-08

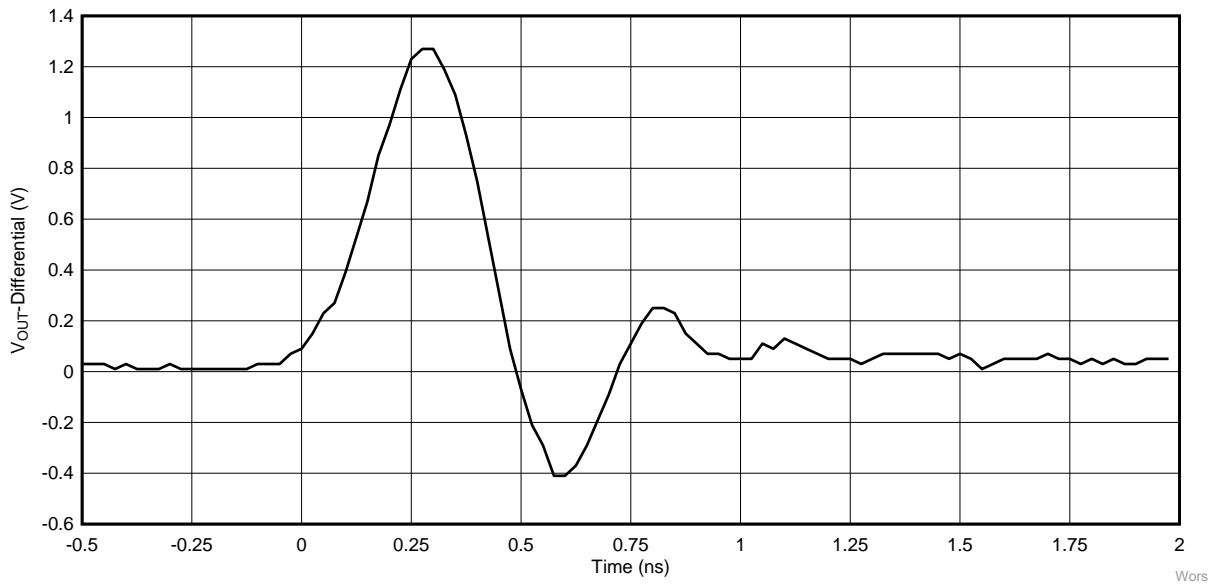
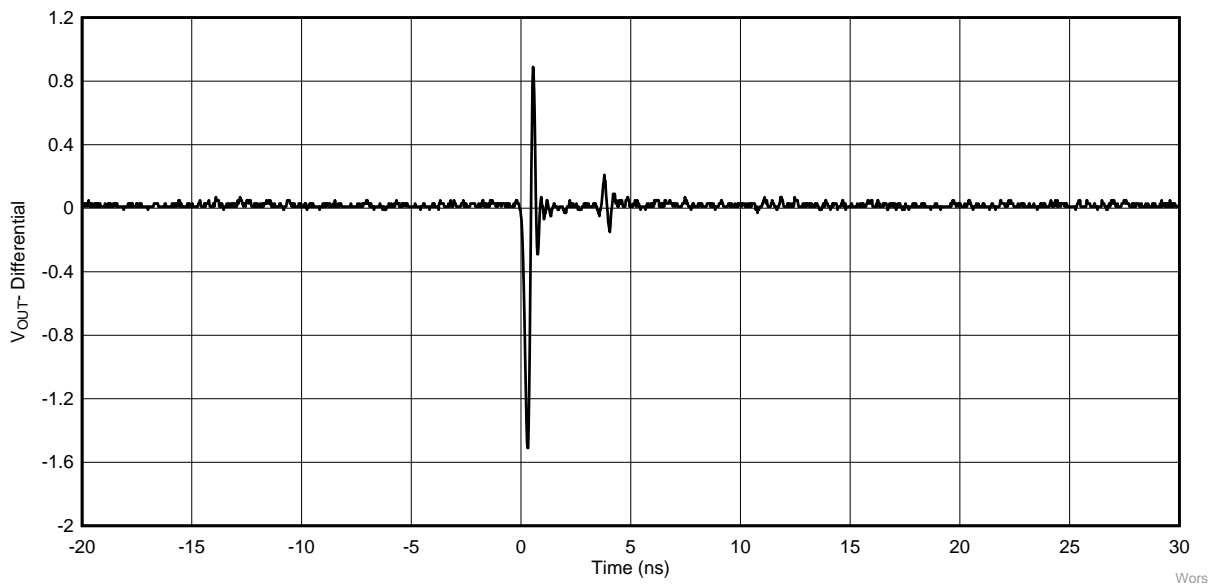


Figure 8. Worst Case Positive Voltage Excursion Upset on Run # 13 at LET_{EFF} = 83.21 MeV-cm²/mg



This upset shows a smaller upset embedded on the data record. This kind of upset was counted as two and each one was properly addressed for histograms purposes. This behavior was rarely seen and only happened when the differential upset was greater than the recommended max voltage of 1 V_{p-p}.

Figure 9. Worst Case Negative Voltage Excursion Upset on Run # 23 at LET_{EFF} = 83.21 MeV-cm²/mg

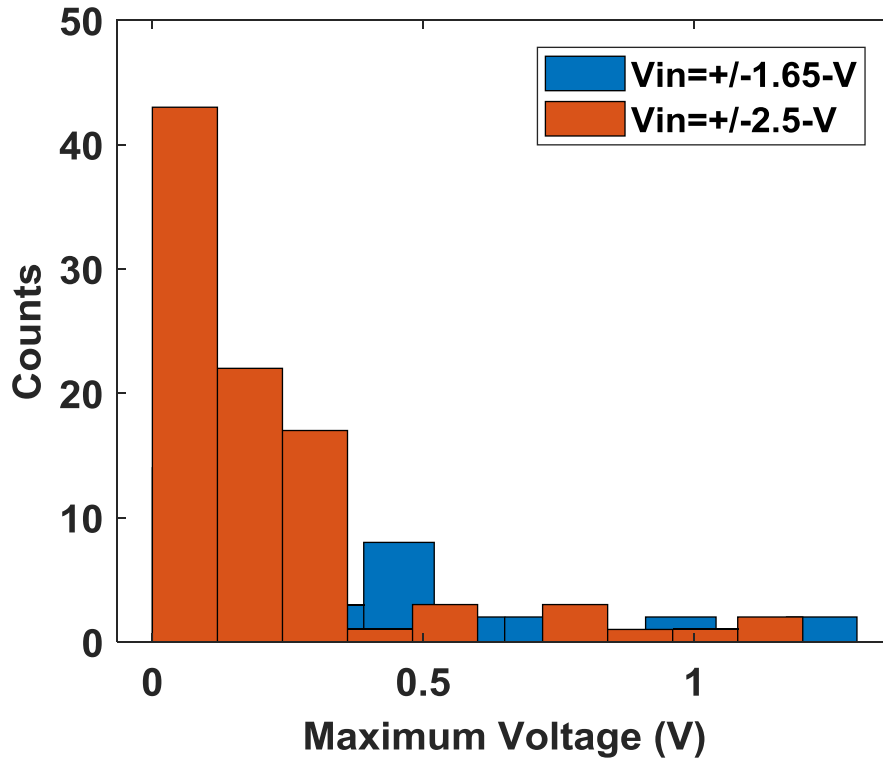


Figure 10. Histogram of the Maximum Voltage for Each Upset Recorded

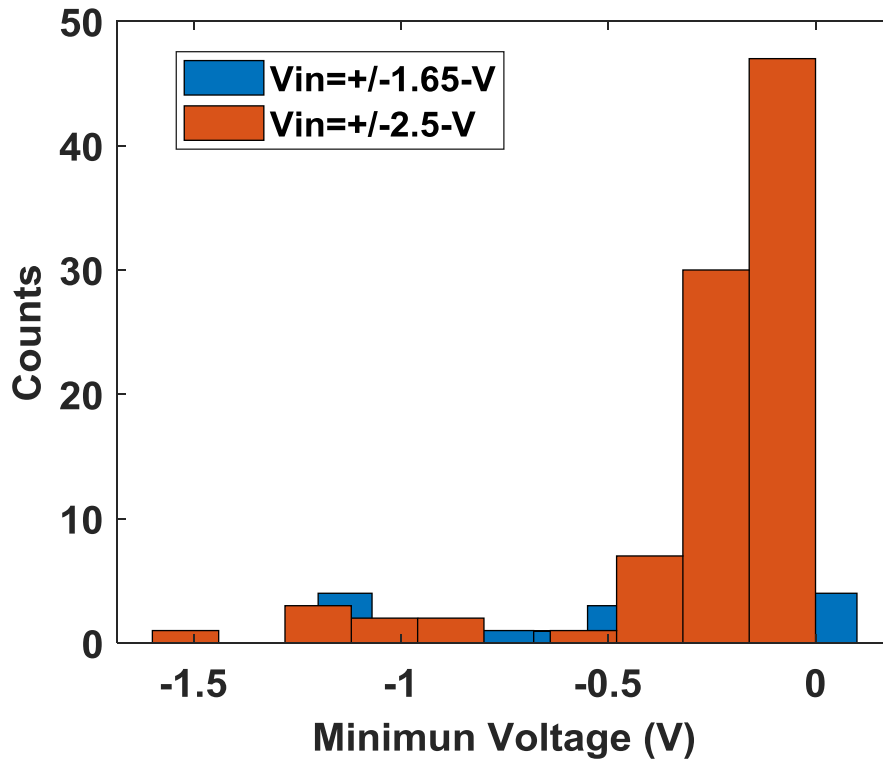


Figure 11. Histogram of the Minimum Voltage for Each Upset Recorded

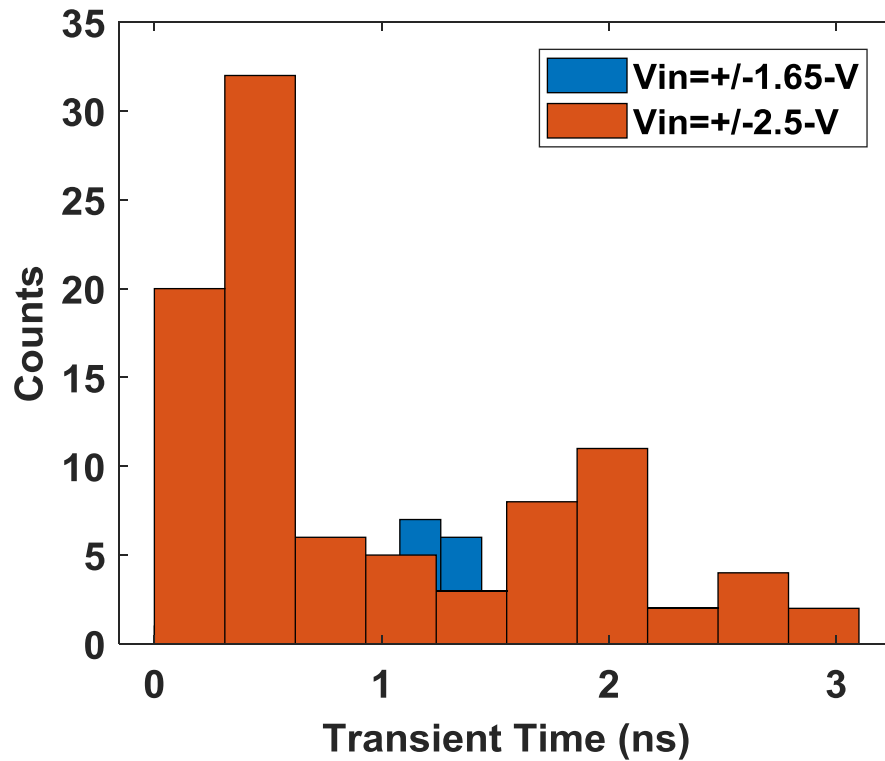


Figure 12. Histogram of the Transient Recovery Time for Each Upset Recorded

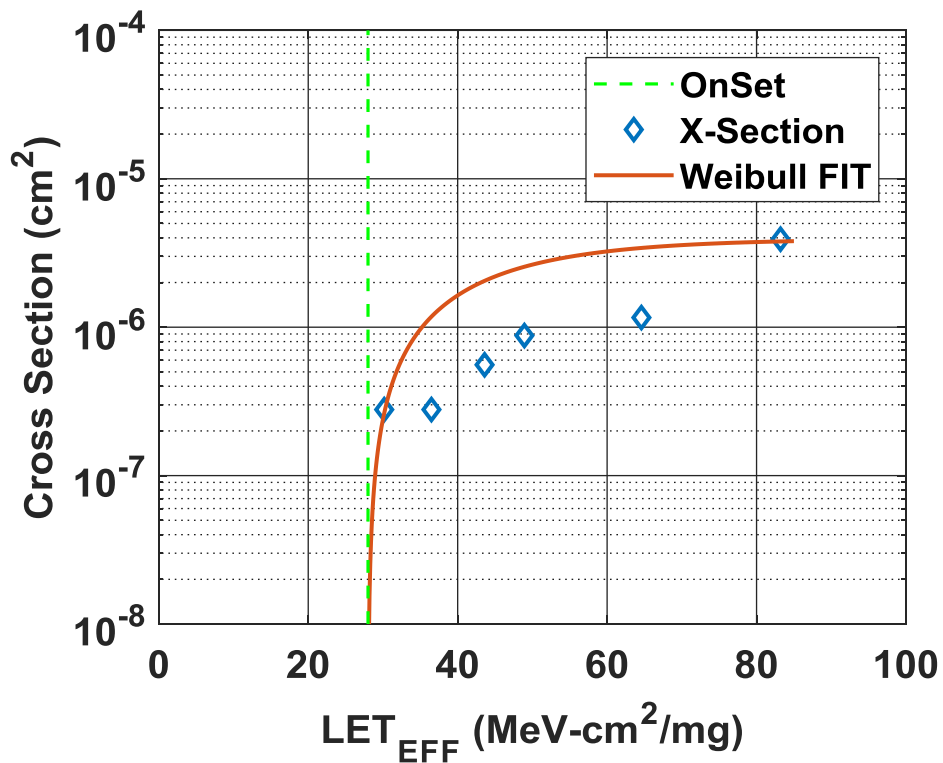


Figure 13. Cross Section and Weibull-Fit for the DC Test at Supply Voltages of ±1.65 V

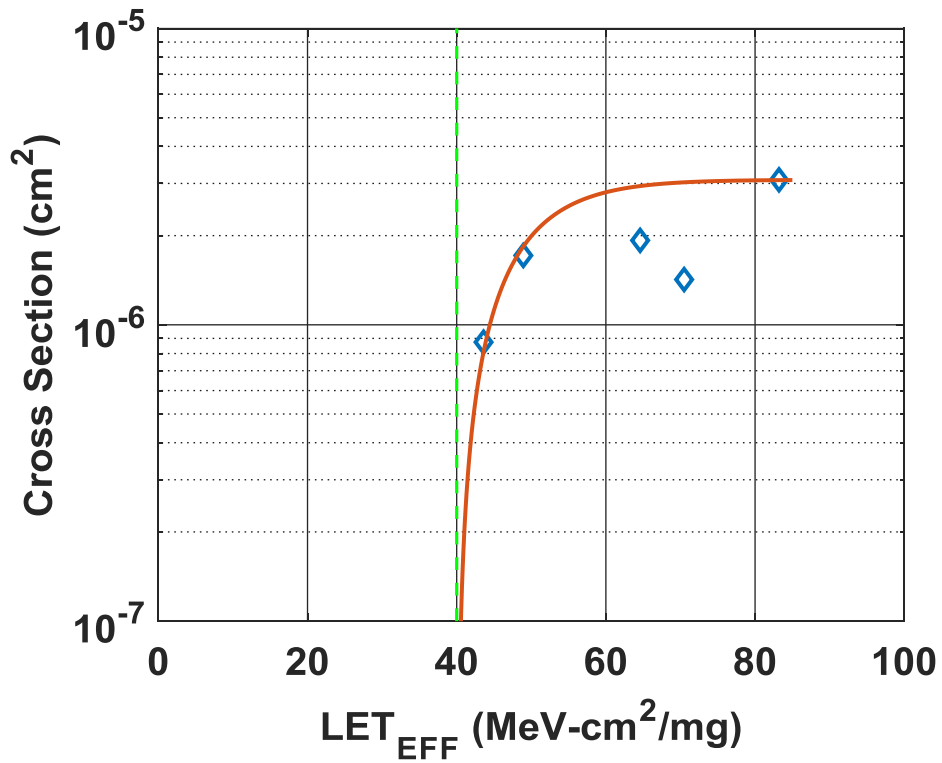


Figure 14. Cross Section and Weibull-Fit for the DC Test at Supply Voltages of ±2.5 V

$$\sigma = \sigma_{SAT} \cdot \left(1 - e^{-\left(\frac{LET - Onset}{W}\right)^s} \right) \tag{2}$$

Table 9. Weibull-FIT Parameters for DC Test at Supply Voltages of ±1.65 and ±2.5 V

Parameter	Supply Voltage = ±1.65 V	Supply Voltage = ±2.5 V
Onset (MeV-cm ² /mg)	28	40
σ _{SAT} (cm ²)	3.92 × 10 ⁻⁶	3.09 × 10 ⁻⁶
W	20	9.7
s	1.2	1.2

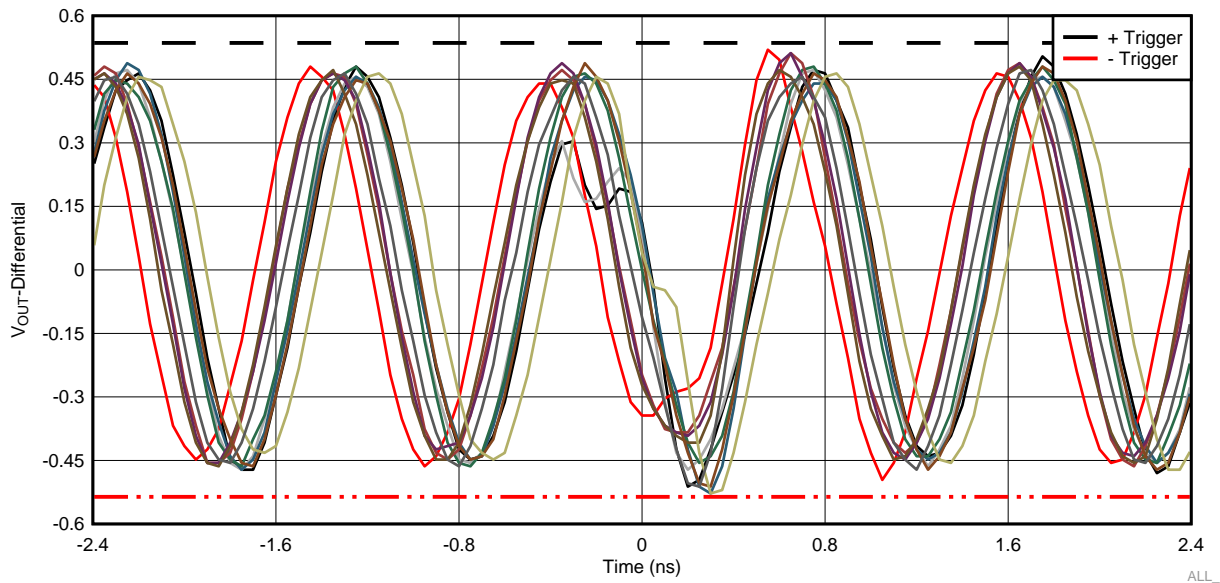


Figure 15. All V_{OUT} -Differential AC Upsets

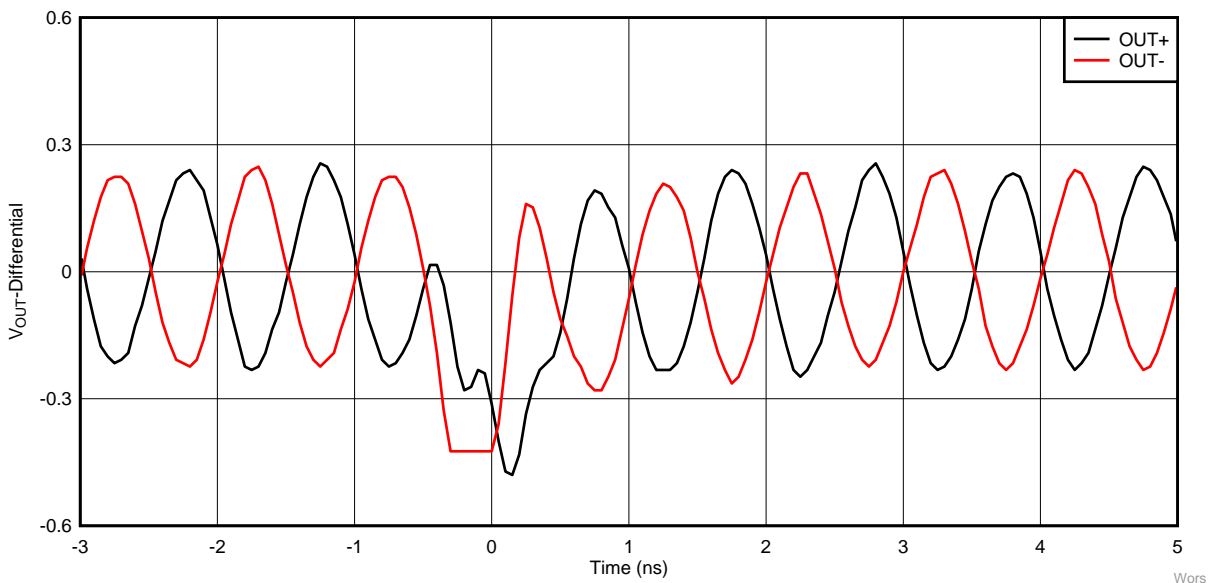


Figure 16. Worst Case Upset on AC Mode When Monitoring Each Output Leg of the LMH5401-SP Separately

9 Event Rate Calculations

Event rates were calculated for LEO (ISS) and GEO environments by combining CREME96 orbital integral flux estimations and simplified SEE cross-sections according to methods described in [Appendix C](#). We assume a minimum shielding configuration of 100 mils (2.54 mm) of aluminum, and “worst-week” solar activity (this is similar to a 99% upper bound for the environment). Using the 95% upper-bounds for the SEL, SET DC at supply voltage of ± 1.65 and SET DC at supply voltage of ± 2.5 the event-rates of the LMH5401-SP are tabulated in [Table 10](#), [Table 11](#), and [Table 12](#).

Table 10. SEL Event Rate Calculations for Worst-Week LEO and GEO Orbits

Orbit Type	Onset LET (MeV·cm ² /mg)	CREME96 Integral Flux (/day·cm ²)	σ_{SAT} (cm ²)	Event Rate (/day)	Event Rate (FIT)	MTBE (Years)
LEO (ISS)	83.2	3.13×10^{-5}	1.23×10^{-7}	3.85×10^{-12}	1.06×10^{-4}	7.12×10^8
GEO		8.78×10^{-5}		1.08×10^{-11}	4.50×10^{-4}	2.54×10^8

Table 11. SET Event Rate Calculations DC ± 1.65 Supply Voltage for Worst-Week LEO and GEO Orbits

Orbit Type	Onset LET (MeV·cm ² /mg)	CREME96 Integral Flux (/day·cm ²)	σ_{SAT} (cm ²)	Event Rate (/day)	Event Rate (FIT)	MTBE (Years)
LEO (ISS)	28.0	2.62×10^{-1}	3.92×10^{-6}	1.03×10^{-6}	42.75	2670.259
GEO		2		7.84×10^{-6}	326.51	349.6194

Table 12. SET Event Rate Calculations DC ± 2.5 Supply Voltage for Worst-Week LEO and GEO Orbits

Orbit Type	Onset LET (MeV·cm ² /mg)	CREME96 Integral Flux (/day·cm ²)	σ_{SAT} (cm ²)	Event Rate (/day)	Event Rate (FIT)	MTBE (Years)
LEO (ISS)	40.0	8.33×10^{-4}	3.09×10^{-6}	2.57×10^{-9}	0.11	1.06×10^6
GEO		2.97×10^{-3}		9.17×10^{-9}	0.38	2.99×10^5

10 Summary

The purpose of this study was to characterize the effect of heavy-ion irradiation on the single-event effect (SEE) performance of the LMH5401-SP 8-GHz, Low Noise, Low Power, Fully-Differential Amplifier. Extensive SEE testing with heavy-ions having LET_{EFF} from 25.4 to 83.21 MeV·cm²/mg were conducted with heavy-ion fluences ranging from 10⁶ to 10⁷ ions/cm² per run, at two different voltages and input conditions. The SEE results demonstrated that the LMH5401-SP is SEL-free up to LET_{EFF} = 83.21 MeV·cm²/mg. Also the SET cross sections are discussed for two supply voltages and under static and dynamic input conditions. Worst case happen to be the DC input condition at supply voltage of 1.65 V. CREME96-based worst-week event-rate calculations for LEO(ISS) and GEO orbits clearly demonstrate the robustness of the LMH5401-SP in two harshly conservative space environments.

Total Ionizing Dose from SEE Experiments

The production LMH5401-SP POL is rated to a total ionizing dose (TID) of 100 krad(Si). In the course of the SEE testing, the heavy-ion exposures delivered ≈ 1 krad(Si) per 10^6 ions/cm² run. The cumulative TID exposure for each device respectively, over all runs they each underwent, was determined to be greater than 100 krad(Si). The two production LMH5401-SP devices used in the studies described in this report stayed within specification and were fully-functional after the heavy-ion SEE testing was completed

Confidence Interval Calculations

For conventional products where hundreds of failures are seen during a single exposure, one can determine the average failure rate of parts being tested in a heavy-ion beam as a function of fluence with high degree of certainty and reasonably tight standard deviation, and thus have a good deal of confidence that the calculated cross-section is accurate.

With radiation hardened parts however, determining the cross-section becomes more difficult since often few, or even, no failures are observed during an entire exposure. Determining the cross-section using an average failure rate with standard deviation is no longer a viable option, and the common practice of assuming a single error occurred at the conclusion of a null-result can end up in a greatly underestimated cross-section.

In cases where observed failures are rare or non-existent, the use of confidence intervals and the chi-squared distribution is indicated. The Chi-Squared distribution is particularly well-suited for the determination of a reliability level when the failures occur at a constant rate. In the case of SEE testing, where the ion events are random in time and position within the irradiation area, one expects a failure rate that is independent of time (presuming that parametric shifts induced by the total ionizing dose do not affect the failure rate), and thus the use of chi-squared statistical techniques is valid (since events are rare an exponential or Poisson distribution is usually used).

In a typical SEE experiment, the device-under-test (DUT) is exposed to a known, fixed fluence (ions/cm²) while the DUT is monitored for failures. This is analogous to fixed-time reliability testing and, more specifically, time-terminated testing, where the reliability test is terminated after a fixed amount of time whether or not a failure has occurred (in the case of SEE tests fluence is substituted for time and hence it is a fixed fluence test) [5]. Calculating a confidence interval specifically provides a range of values which is likely to contain the parameter of interest (the actual number of failures/fluence). Confidence intervals are constructed at a specific confidence level. For example, a 95% confidence level implies that if a given number of units were sampled numerous times and a confidence interval estimated for each test, the resulting set of confidence intervals would bracket the true population parameter in about 95% of the cases.

In order to estimate the cross-section from a null-result (no fails observed for a given fluence) with a confidence interval, we start with the standard reliability determination of lower-bound (minimum) mean-time-to-failure for fixed-time testing (an exponential distribution is assumed):

$$MTTF = \frac{2nT}{\chi^2_{2(d+1); 100\left(1-\frac{\alpha}{2}\right)}} \tag{3}$$

Where *MTTF* is the minimum (lower-bound) mean-time-to-failure, *n* is the number of units tested (presuming each unit is tested under identical conditions) and *T*, is the test time, and χ^2 is the chi-square distribution evaluated at 100 (1 – σ / 2) confidence level and where *d* is the degrees-of-freedom (the number of failures observed). With slight modification for our purposes we invert the inequality and substitute *F* (fluence) in the place of *T*:

$$MFTF = \frac{2nF}{\chi^2_{2(d+1); 100\left(1-\frac{\alpha}{2}\right)}} \tag{4}$$

Where now *MFTF* is mean-fluence-to-failure and *F* is the test fluence, and as before, χ^2 is the chi-square distribution evaluated at 100 $(1 - \sigma / 2)$ confidence and where *d* is the degrees-of-freedom (the number of failures observed). The inverse relation between MTTF and failure rate is mirrored with the MFTF. Thus the upper-bound cross-section is obtained by inverting the MFTF:

$$\sigma = \frac{\chi^2_{2(d+1); 100\left(1-\frac{\sigma}{2}\right)}}{2nF} \quad (5)$$

Let's assume that all tests are terminated at a total fluence of 10^6 ions/cm². Let's also assume that we have a number of devices with very different performances that are tested under identical conditions. Assume a 95% confidence level ($\sigma = 0.05$). Note that as *d* increases from 0 events to 100 events the actual confidence interval becomes smaller, indicating that the range of values of the true value of the population parameter (in this case the cross-section) is approaching the mean value + 1 standard deviation. This makes sense when one considers that as more events are observed the statistics are improved such that uncertainty in the actual device performance is reduced.

Table 13. Experimental Example Calculation of Mean-Fluence-to-Failure (MFTF) and σ Using a 95% Confidence Interval⁽¹⁾

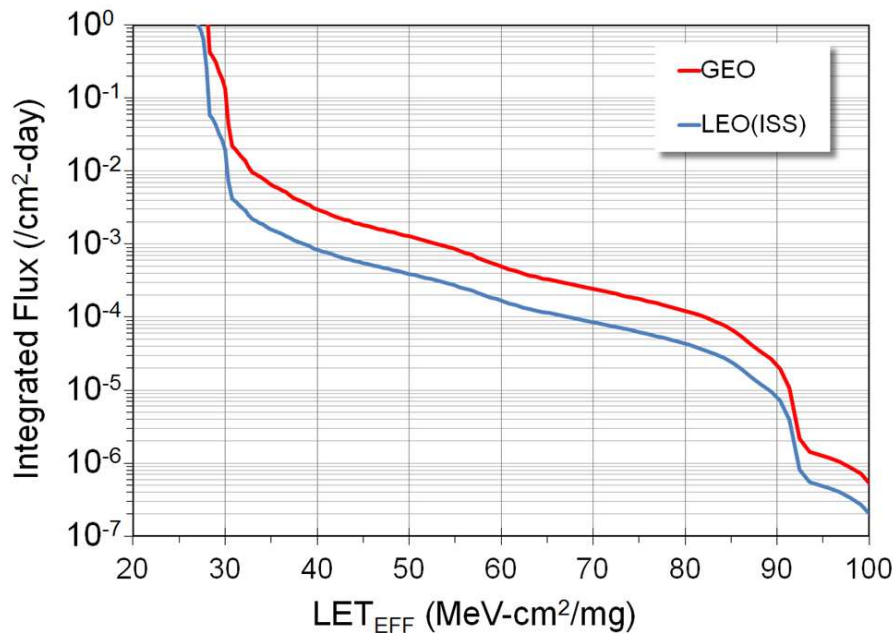
Degrees-of-Freedom (d)	2(d + 1)	χ^2 @ 95%	Calculated Cross-Section (cm ²)		
			Upper-Bound @ 95% Confidence	Mean	Average + Standard Deviation
0	2	7.38	3.69E-06	0.00E+00	0.00E+00
1	4	11.14	5.57E-06	1.00E-06	2.00E-06
2	6	14.45	7.22E-06	2.00E-06	3.41E-06
3	8	17.53	8.77E-06	3.00E-06	4.73E-06
4	10	20.48	1.02E-05	4.00E-06	6.00E-06
5	12	23.34	1.17E-05	5.00E-06	7.24E-06
10	22	36.78	1.84E-05	1.00E-05	1.32E-05
50	102	131.84	6.59E-05	5.00E-05	5.71E-05
100	202	243.25	1.22E-04	1.00E-04	1.10E-04

⁽¹⁾ Using a 99% confidence for several different observed results (d = 0, 1, 2, and 3 observed events during fixed-fluence tests) on four identical devices and test conditions.

Orbital Environment Estimations

In order to calculate on-orbit SEE event rates one needs both the device SEE cross-section and the flux of particles encountered in a particular orbit. Device SEE cross-sections are usually determined experimentally while flux of particles in orbit is calculated using various codes. For the purpose of generating some event rates, a Low-Earth Orbit (LEO) and a Geostationary-Earth Orbit (GEO) were calculated using CREME96. CREME96 code, short for Cosmic Ray Effects on Micro-Electronics is a suite of programs [6][7] that enable estimation of the radiation environment in near-Earth orbits. CREME96 is one several tools available in the aerospace industry to provide accurate space environment calculations. Over the years since its introduction, the CREME models have been compared with on-orbit data and demonstrated their accuracy. In particular, CREME96 incorporates realistic “worst-case” solar particle event models, where fluxes can increase by several orders-of-magnitude over short periods of time.

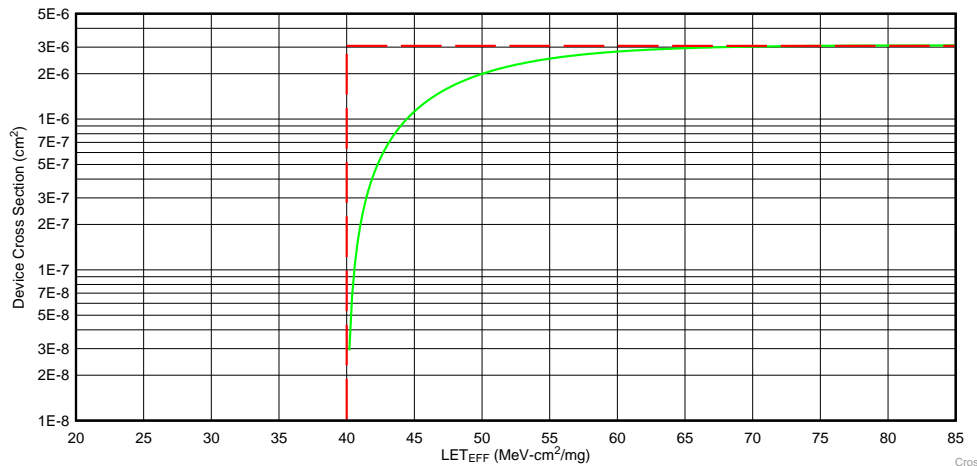
For the purposes of generating conservative event rates, the worst-week model (based on the biggest solar event lasting a week in the last 45 years) was selected, which has been equated to a 99%-confidence level worst-case event [8][9]. The integrated flux includes protons to heavy ions from solar and galactic sources. A minimal shielding configuration is assumed at 100 mils (2.54 mm) of aluminum. Two orbital environments were estimated, that of the International Space Station (ISS), which is LEO, and the GEO environment. Figure 17 shows the integrated flux (from high LET to low) for these two environments.



- (1) LEO(ISS) (blue) and a GEO (red) environment as calculated by CREME96 assuming worst-week and 100 mils (2.54 mm) of aluminum shielding.

Figure 17. Integral Particle Flux vs LET_{EFF}

Using this data, we can extract integral particle fluxes for any arbitrary LET of interest. To simplify the calculation of event rates we assume that all cross-section curves are square – meaning that below the onset LET the cross-section is identically zero while above the onset LET the cross-section is uniformly equal to the saturation cross-section. Figure 18 illustrates the approximation, with the green curve being the actual Weibull fit to the data with the “square” approximation shown as the red-dashed line. This allows us to calculate event rates with a single multiplication, the event rate becoming simply the product of the integral flux at the onset LET, and the saturation cross-section. Obviously this leads to an over-estimation of the event rate since the area under the square approximation is larger than the actual cross-section curve – but for the purposes of calculating upper-bound event rate estimates, this modification avoids the need to do the integral over the flux and cross-section curves.



- (1) Weibull Fit (green) is “simplified” with the use of a square approximation (red dashed line).

Figure 18. Device Cross-Section vs LET_{EFF}

To demonstrate how the event rates in this report were calculated, assume that we wish to calculate an event rate for a GEO orbit for the device whose cross-section is shown in Figure 18. Using the red curve in Figure 17 and the onset LET value obtained from Figure 18 (~ 40 MeV-cm²/mg) we find the GEO integral flux to be ~ 2.97 × 10⁻³ ions/cm²-day. The event rate is the product of the integral flux and the saturation cross-section in Figure 18 (~ 3.09 × 10⁻⁶ cm²):

$$GEO \text{ Event Rate} = \left(2.97 \times 10^{-3} \frac{\text{ions}}{\text{cm}^2 \times \text{day}} \right) \times (3.09 \times 10^{-6} \text{ cm}^2) = 9.17 \times 10^{-9} \frac{\text{events}}{\text{day}} \quad (6)$$

$$GEO \text{ Event Rate} = 3.82 \times 10^{-10} \frac{\text{events}}{\text{hr}} = 0.382 \text{ FIT} \quad (7)$$

$$MTBF = 298901 \text{ Years !} \quad (8)$$

References

- (1) M. Shoga and D. Binder, "Theory of Single Event Latchup in Complementary Metal-Oxide Semiconductor ICs", IEEE Trans. Nucl. Sci., 33(6), Dec. 1986, pp. 1714-1717.
- (2) G. Bruguier and J.M. Palau, "Single particle-induced latchup", IEEE Trans. Nucl. Sci, Vol. 43(2), Mar. 1996, pp. 522-532.
- (3) TAMU Radiation Effects Facility website. <http://cyclotron.tamu.edu/ref/>
- (4) "The Stopping and Range of Ions in Matter" (SRIM) software simulation tools website. <http://www.srim.org/index.htm#SRIMMENU>
- (5) D. Kececioglu, "Reliability and Life Testing Handbook", Vol. 1, PTR Prentice Hall, New Jersey, 1993, pp. 186-193.
- (6) <https://creme.isde.vanderbilt.edu/CREME-MC>
- (7) A. J. Tylka, et al., "CREME96: A Revision of the Cosmic Ray Effects on Micro-Electronics Code", IEEE Trans. Nucl. Sci., 44(6), 1997, pp. 2150-2160.
- (8) A. J. Tylka, W. F. Dietrich, and P. R. Bobery, "Probability distributions of high-energy solar-heavy-ion fluxes from IMP-8: 1973-1996", IEEE Trans. on Nucl. Sci., 44(6), Dec. 1997, pp. 2140 – 2149.
- (9) A. J. Tylka, J. H. Adams, P. R. Bobery, et al., "CREME96: A Revision of the Cosmic Ray Effects on Micro-Electronics Code", Trans. on Nucl. Sci, 44(6), Dec. 1997, pp. 2150 – 2160.

IMPORTANT NOTICE AND DISCLAIMER

TI PROVIDES TECHNICAL AND RELIABILITY DATA (INCLUDING DATASHEETS), DESIGN RESOURCES (INCLUDING REFERENCE DESIGNS), APPLICATION OR OTHER DESIGN ADVICE, WEB TOOLS, SAFETY INFORMATION, AND OTHER RESOURCES "AS IS" AND WITH ALL FAULTS, AND DISCLAIMS ALL WARRANTIES, EXPRESS AND IMPLIED, INCLUDING WITHOUT LIMITATION ANY IMPLIED WARRANTIES OF MERCHANTABILITY, FITNESS FOR A PARTICULAR PURPOSE OR NON-INFRINGEMENT OF THIRD PARTY INTELLECTUAL PROPERTY RIGHTS.

These resources are intended for skilled developers designing with TI products. You are solely responsible for (1) selecting the appropriate TI products for your application, (2) designing, validating and testing your application, and (3) ensuring your application meets applicable standards, and any other safety, security, or other requirements. These resources are subject to change without notice. TI grants you permission to use these resources only for development of an application that uses the TI products described in the resource. Other reproduction and display of these resources is prohibited. No license is granted to any other TI intellectual property right or to any third party intellectual property right. TI disclaims responsibility for, and you will fully indemnify TI and its representatives against, any claims, damages, costs, losses, and liabilities arising out of your use of these resources.

TI's products are provided subject to TI's Terms of Sale (www.ti.com/legal/termsofsale.html) or other applicable terms available either on ti.com or provided in conjunction with such TI products. TI's provision of these resources does not expand or otherwise alter TI's applicable warranties or warranty disclaimers for TI products.

Mailing Address: Texas Instruments, Post Office Box 655303, Dallas, Texas 75265
Copyright © 2018, Texas Instruments Incorporated